

**Defective fullerenes and nanotubes as molecular magnets: An *ab initio* study**

Yong-Hyun Kim,\* Jin Choi, and K. J. Chang†

*Department of Physics, Korea Advanced Institute of Science and Technology, Daejeon 305-701, Korea*

David Tománek‡

*Department of Physics and Astronomy, Michigan State University, East Lansing, Michigan 48824-2320, USA*

(Received 13 February 2003; revised manuscript received 3 July 2003; published 26 September 2003)

Using *ab initio* spin-density-functional calculations, we investigate the electronic and magnetic structures of a  $C_{60}$  fullerene during a structural transition to a nanotube segment by a series of Stone-Wales transformations. We find that partly opened intermediate cage structures may acquire a magnetic moment of several Bohr magnetons. Our results offer a possible explanation for the ferromagnetic behavior observed in polymerized  $C_{60}$  following exposure to high temperatures and pressures, and suggest the use of carbon nanostructures for magnetic measurements.

DOI: 10.1103/PhysRevB.68.125420

PACS number(s): 61.48.+c, 64.70.Nd, 75.75.+a, 73.22.-f

Carbon nanostructures are emerging as new, fascinating magnetic materials that are both fundamentally interesting and offer a large variety of technological applications.<sup>1</sup> Even though the fundamental mechanism and the structural units responsible for the ferromagnetic ordering are not well established, the experimental evidence for ferromagnetic carbon nanostructures appears to be firm. In this paper, based on *ab initio* spin-density-functional calculations, we identify all-carbon nanostructures, related to fullerenes and nanotubes with a particular arrangement of undercoordinated carbon atoms, as potential molecular magnets.

Our study was partly motivated by the recent discovery of a room-temperature all-carbon magnet consisting of polymerized  $C_{60}$  molecules.<sup>2,3</sup> Although this finding is a significant step in the long-standing search for novel high-temperature magnets,<sup>4</sup> the origin of this magnetic behavior has not been established yet. The magnetic carbon samples were prepared<sup>2</sup> by exposing solid  $C_{60}$  to a pressure of 6 GPa and a temperature of 1000 K, which are close to, but below, the stability limit of the fullerene cage. The fullerene cage was found to collapse easily above 1000 K, followed by graphitization. The observation of magnetic carbons was later confirmed<sup>3</sup> for samples grown at a higher pressure of 9 GPa and lower temperature of 800 K. Under these higher pressures, the carbon cage starts collapsing above 850 K. In both experiments, the preparation temperature for magnetic samples lies in a narrow window just below the stability limit of the cage structure.

From measured concentrations of transition-metal impurities, Makarova *et al.* conjectured that these impurities play only a minor role in the magnetic behavior, and suggested a possible link between magnetism and defects in the pure carbon network, such as unpaired  $\sigma$  electrons. Very recently, a theoretical attempt<sup>5</sup> has been made to understand the peculiar magnetic behavior on the basis of vacancy-mediated  $sp^2$ - $sp^3$  hybridization. However, an ambiguity still remains in the vacancy model, because the magnetism is very sensitive to the preparation time. Even magnetic samples, which were properly prepared, were shown to turn nonmagnetic upon annealing at 700 K for several hours, indicating that the magnetic samples may be intermediate metastable structures

with a finite lifetime. Defects rather than impurities may also be the source of transient ferromagnetism observed in  $C_{60}H_{24}$  hydrofullerites after a high-pressure synthesis.<sup>6</sup>

In this work we focus on defective  $sp^2$  bonded carbon nanostructures with unsaturated  $\sigma$  dangling bonds. We find that new metastable isomer states of  $C_{60}$  may form during the cage opening process, which can occur under the experimental extreme conditions. A zigzag arrangement of edge atoms in the defective cage creates dangling bonds, which in turn lead to magnetic instabilities in isolated molecules and even ferromagnetism in the solid.<sup>7</sup> A similar arrangement of carbon atoms at the unsaturated edge of a zigzag nanotube may give rise to magnetic moments of up to one Bohr magneton,  $\mu_B$ , per unsaturated dangling bond. We found a magnetic moment close to  $10\mu_B$  associated with the open edge of a (10,0) nanotube, suggesting the use of such open-ended tubes as magnetic scanning probe microscopy tips.

All the calculations are performed within the spin-polarized density-functional formalism,<sup>8,9</sup> using the generalized gradient correction<sup>10</sup> for the exchange-correlation functional. Carbon atoms are represented by ultrasoft pseudopotentials.<sup>11</sup> In a periodic structure, isolated molecules are arranged on a superlattice with sufficiently large unit cells, which guarantee a minimum separation of 6 Å between closest atoms in noninteracting structures. We use a plane-wave basis with a kinetic-energy cutoff of 28 Ry. During structure optimization, we relax the ionic coordinates until the Hellmann-Feynman forces are less than 2.8 mRy/Å. Using this approach, we achieve a total energy precision of less than 1 meV per  $C_{60}$  molecule.

Opening the  $C_{60}$  cage can be achieved by a sequence of Stone-Wales (SW) transformations,<sup>12</sup> which can be viewed as bond rotations and require less energy than bond breaking. As shown in Fig. 1, a sequence of only five SW-type bond rotations transforms a perfect  $C_{60}$  molecule to a capped segment of a (5,5) nanotube. The intermediate open cage structures, occurring sequentially during the stepwise transformation process, are labeled as SW-I, SW-II, SW-III, and S(5,5). The transition from SW-III to S(5,5) involves two SW transformations that occur in parallel. In the SW-I and SW-II systems, two dangling bonds form in the zigzag geometry of

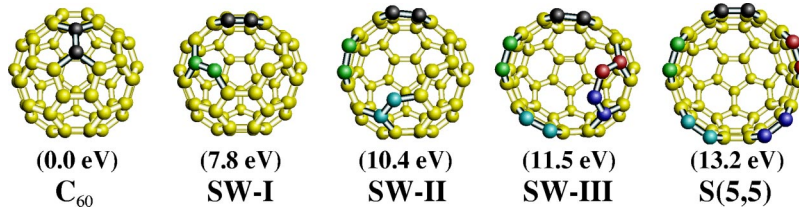


FIG. 1. (Color online) Ball-and-stick models of intermediate structures occurring during the transformation of a  $C_{60}$  molecule to a capped segment of a (5,5) nanotube. The metastable open cage structures occurring sequentially during the stepwise Stone-Wales transformation process are labeled as SW-I, SW-II, and SW-III. Atoms involved in Stone-Wales bond rotations are identified by different colors. The  $C_{60}$ , SW-III, and S(5,5) structures are nonmagnetic, SW-I is ‘antiferromagnetic’, and SW-II is ‘ferromagnetic’. Numbers in parentheses indicate the total energies of the isomers relative to the  $C_{60}$  molecule.

twofold coordinated edge atoms. As expected, energy investment is required to open the cage, which increases the number of undercoordinated atoms. Transformation of the perfect  $C_{60}$  molecule to the SW-I structure requires a relatively large energy of 7.8 eV, since the latter structure has lost two single bonds during the SW-type rotation. Subsequent Stone-Wales transformations require less than 3 eV, since they reduce the number of single bonds by only one per bond rotation. Previous tight-binding calculations<sup>13</sup> showed that a minimum energy of 0.3 eV is required to change the structure of SW-I, implying that the SW-I isomer maintains its stability at room temperature.

Even though the intermediate structures are energetically less favorable, they are all metastable and exhibit a very peculiar magnetic behavior. Our calculations confirm the known fact that the perfect  $C_{60}$  is nonmagnetic. Rather surprisingly, we find that the SW-III and S(5,5) structures are also nonmagnetic, even though they contain undercoordinated carbon atoms. It turns out that  $sp^2$  structures with a local armchair termination reconstruct, converting double bonds at the edge to triple bonds. This reconstruction eliminates dangling bonds at the edge, thus chemically passivating the system. Indeed, we find the bond lengths of about 1.24 Å near the armchair edge of the SW-III and S(5,5) structures to match the C-C triple bond length in  $C_2H_2$ , 1.20 Å, much more closely than the C-C double bond length in  $C_2H_4$ , 1.34 Å. At a zigzag edge, the situation is different, since dangling bonds cannot be saturated by reconstruction, leaving unpaired spins behind. We find that such structures can acquire a net magnetic moment.

Our spin-polarized calculations identify magnetic solutions with different spin arrangements. For the sake of convenience, we will call solutions with a nonzero net magnetic moment and all spins aligned “ferromagnetic,” and solutions with alternating spin directions and a vanishing net magnetic moment “antiferromagnetic.” Energy differences between the ferromagnetic (FM) and the antiferromagnetic (AF) state are discussed in Table I.

We find that in the ground state, antiferromagnetic ordering is favored by 36 meV with respect to a ferromagnetic spin configuration for the SW-I structure. In the SW-II structure, we find the ferromagnetic configuration favored over the antiferromagnetic state by 10 meV. In the latter system, the net magnetic moment of about  $2\mu_B$  results from one spin per zigzag dangling bond. Since all valence electrons at the four undercoordinated edge atoms with armchair-type align-

ment participate in covalent bonds, they do not contribute to the magnetic moment.

To understand why SW-I is antiferromagnetic, whereas SW-II is ferromagnetic in the ground state, we compare the spin distribution for the different magnetic solutions. Figure 2 depicts isosurfaces of the spin density  $\Delta n(\mathbf{r})$ , defined by  $\Delta n(\mathbf{r}) = n_{\uparrow}(\mathbf{r}) - n_{\downarrow}(\mathbf{r})$ , where  $n_{\uparrow}$  is the spin-up and  $n_{\downarrow}$  the spin-down density. As expected, the spin density is largest near carbon atoms with dangling bonds at the zigzag edge. In the SW-I structure, the two clouds of unpaired electrons appear closer to each other than in the SW-II structure. Due to the larger overlap between the electron clouds in the SW-I structure, the antiferromagnetic configuration is preferred energetically. In the SW-II structure, on the other hand, the lower degree of overlap between the electron clouds stabilizes the ferromagnetic configuration.

Our results suggest that adjacent dangling bonds at a zigzag edge, found in the SW-II structure, may be considered a basic element responsible for ferromagnetic ordering in  $sp^2$  bonded carbon nanostructures. This is consistent with previous results suggesting the formation of a partly filled flat band, causing a magnetic instability at the zigzag edge of graphitic ribbons.<sup>14</sup> For a ribbon, however, the total magnetic moment vanishes, because its two zigzag edges couple anti-

TABLE I. Total energy difference  $E_{FM} - E_{AF}$  between the ferromagnetic and antiferromagnetic spin configurations for metastable isomers of  $C_{60}$  described in Fig. 1, and for nanotube segments shown in Fig. 3. The total magnetic moment  $\mu$  is given for ferromagnetic systems. Values in parentheses indicate the magnetic moment per zigzag-type dangling bond.

System	$E_{FM} - E_{AF}$ (meV)	$\mu$ ( $\mu_B$ )
$C_{60}$	0	
SW-I	36	
SW-II	-10	2.06 (1.03)
SW-III	0	
S(5,5)	0	
(8,0) Tube (capped)	-71	10.0 (1.25)
(8,0) Tube (unterminated)	132	
(8,0) Tube (hydrogenated)	-130	8.0 (1.00)
(10,0) Tube (capped)	-49	10.48 (1.05)
(10,0) Tube (unterminated)	903	
(10,0) Tube (hydrogenated)	-275	10.12 (1.01)

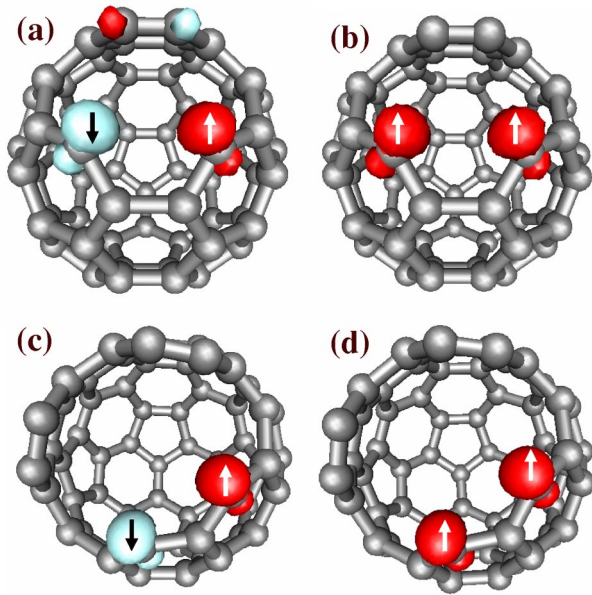


FIG. 2. (Color online) Spin-density isosurfaces for the antiferromagnetic and ferromagnetic spin configurations of the SW-I and SW-II isomers: (a) antiferromagnetic SW-I, (b) ferromagnetic SW-I, (c) antiferromagnetic SW-II, and (d) ferromagnetic SW-II. Red-dark (blue-white) isosurfaces represent equal densities of spin-up (spin-down) electrons, as indicated by arrows.

ferromagnetically. Recently, ferromagnetic ordering was also proposed at zigzag edges of graphene sheets, carbon nanotubes, and at BN/C interfaces in doped heterostructured nanotubes.<sup>16,15,17</sup>

It is likely that the ferromagnetic behavior observed in solid  $C_{60}$ , polymerized under very high temperatures and pressures,<sup>2,3</sup> may be related to atomic defects. This conjecture appears especially plausible in view of the fact that the observed magnetization, corresponding to less than one unpaired spin per thousands of atoms, is very small. Among the defects, we believe that unsaturated zigzag edges are much more likely candidates to cause this magnetic behavior than other defects, including atomic vacancies. The high-temperature and -pressure conditions during the polymerization process are likely to create both atomic vacancies and metastable  $C_{60}$  isomers, such as those depicted in Fig. 1, at a similar energy cost of about 10 eV.<sup>18</sup> The observation that magnetism of polymerized samples disappears upon annealing to 700 K, however, is easier to explain by the conversion of metastable  $C_{60}$  isomers to a perfect, nonmagnetic structure, than by the presence of vacancies. Even though the study of long-range magnetic ordering is beyond the scope of our calculations, the mere finding of a net magnetic moment in a particular substructure within the SW-II isomer bears promise to support our conjecture that the observed magnetism may originate in partly damaged  $C_{60}$  cages.

In the cage opening process, the SW-II isomer was shown to be magnetically stable with the energy gain of 10 meV with respect to the antiferromagnetic configuration. However, this energy is too small to explain the room-temperature ferromagnetism. Under experimental conditions near the cage stability limit, the cage can be damaged in various

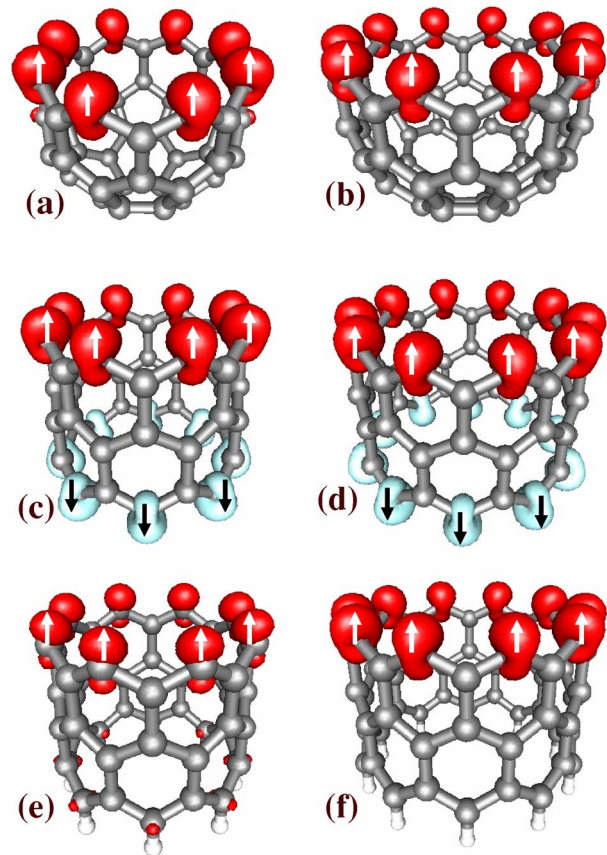


FIG. 3. (Color online) Spin-density isosurfaces for ground-state spin configurations of various (8,0) and (10,0) nanotube segments: dome terminated (a) (8,0) and (b) (10,0) with ferromagnetic ordering; unterminated (c) (8,0) and (d) (10,0) with antiferromagnetic ordering; and hydrogen-passivated (e) (8,0) and (f) (10,0) with ferromagnetic ordering. H atoms are represented by white balls. Red-dark (blue-white) isosurfaces represent equal densities of spin-up (spin-down) electrons, as indicated by arrows.

ways. Since the zigzag arrangement of dangling bonds is important for the occurrence of magnetism, the damage process will be proceeded to maximize the number of zigzag dangling bonds, as shown in zigzag tubes.

Following up on our finding about structures that maximize the net magnetic moment with zigzag dangling bonds, we calculated the magnetic moment in finite segments of (8,0) and (10,0) zigzag carbon nanotubes with different terminations. Our results are summarized in Fig. 3. Nanotubes that were capped from one end, shown in Figs. 3(a) and 3(b), are compared to uncapped nanotube segments with the same number of carbon atoms in Figs. 3(c) and 3(d). Figures 3(e) and 3(f) depict nanotube segments that have been saturated with hydrogen at one end only. Energies for the different spin configurations in these structures are compared in Table I.

We find that the capped segments of the (8,0) and (10,0) zigzag nanotubes favor the ferromagnetically ordered spin configuration by 71 meV and 49 meV, respectively, with respect to the antiferromagnetic spin configuration. These results suggest that open-ended zigzag nanotubes should behave as all-carbon molecular magnets even at room

temperature. Since the latter is a cage-opened isomer of  $C_{60}$ , it is a good, possible candidate for the magnetically stable  $C_{60}$  at room temperature. The magnetic moment per dangling bond in the capped (8,0) segment is calculated to be  $1.25\mu_B$ , which is somewhat higher than in the capped (10,0) nanotube with a smaller curvature. In nanotube segments that are not terminated on either side, the ground state shows an antiferromagnetic configuration, with nonzero net magnetic moments at the edges compensating each other, similar to graphitic ribbons with zigzag edges.<sup>14,15</sup> We conclude that a nonzero net magnetic moment can only be achieved when one of the tube ends is terminated. This can be achieved by a dome, as shown in Figs. 3(a) and 3(b). The net magnetic moment then originates from the dangling bonds at the open edge, which align ferromagnetically.

An alternative way to terminate a nanotube is by passivating the open edges with hydrogen. Zigzag nanotubes that are passivated by hydrogen only at one end, depicted in Figs. 3(e) and 3(f), also strongly favor ferromagnetic spin ordering at the unsaturated edge, as suggested by our results in Table I. The net magnetic moment in zigzag nanotube segments, which are dome terminated or hydrogen passivated from one side, turns out to be  $8.0\mu_B$  in the (8,0) and  $10.1\mu_B$  in the (10,0) tube, corresponding to a magnetic moment  $\mu \approx \mu_B$  per dangling bond. These results also suggest that a net magnetic moment should form at the open edge of long zigzag nano-

tubes, suggesting a possible use of these systems as atomically well-defined tips for use in magnetic scanning probe microscopy. Finally, of special interest is that small  $\pi$ -electron net magnetic moment is observed at the H-passivated nanotube edge in Fig. 3(e).

In conclusion, we have investigated the magnetic ordering in selected metastable isomers of  $C_{60}$  with partly opened cages. We find that a ferromagnetic spin configuration is energetically favorable in isomers with unsaturated dangling bonds at zigzag edges. Such structures are likely to form under synthesis conditions close to the stability limit of the fullerene cage. Thus, identifying  $C_{60}$  isomers with a net magnetic moment may explain the recently observed ferromagnetic behavior of polymerized  $C_{60}$ . We found a very similar magnetic behavior in structurally related segments of carbon nanotubes. Our results suggest the occurrence of very large magnetic moments at the open edge of truncated zigzag carbon nanotubes. We propose a possible use of these systems as atomically well-defined all-carbon tips for magnetic scanning probe microscopy.

This work was supported by the MOST of Korea through the National Science and Technology Program (Grant No. M1-0213-04-0001). One of us (D.T.) acknowledges financial support by the NSF-NIRT Grant No. DMR-0103587. Calculations were done using the PWSCF package.<sup>19</sup>

\*Present address: National Renewable Energy Laboratory, Golden, Colorado 80401; Email address: ykim@nrel.gov

†Email address: kchang@kaist.ac.kr

‡Email address: tomanek@msu.edu

<sup>1</sup>T.L. Makarova, "Magnetism of carbon-based materials," Studies of High-Tc Superconductivity, Vol. 45, 107–169, edited by A. Narlikar (Nova Science Publisher, Huntington, New York, 2003), and references therein.

<sup>2</sup>T.L. Makarova, B. Sundqvist, R. Höhne, P. Esquinazi, Y. Kopelevich, P. Scharff, V.A. Davydov, L.S. Kashevarova, and A.V. Rakhmanina, *Nature (London)* **413**, 716 (2001).

<sup>3</sup>R.A. Wood, M.H. Lewis, M.R. Lees, S.M. Bennington, M.G. Cain, and N. Kitamura, *J. Phys.: Condens. Matter* **14**, L385 (2002).

<sup>4</sup>F. Palacio, *Nature (London)* **413**, 690 (2001), and references therein.

<sup>5</sup>A.N. Andriotis, M. Menon, R.M. Sheetz, and L. Chernozatonskii, *Phys. Rev. Lett.* **90**, 026801 (2003).

<sup>6</sup>V.E. Antonov, I.O. Bashkin, S.S. Khasanov, A.P. Moravsky, Yu.G. Morozov, Yu.M. Shulga, Yu.A. Ossipyan, and E.G. Ponyatovsky, *J. Alloys Compd.* **330**, 365 (2002).

<sup>7</sup>Here we focus on the possible occurrence of a magnetic moment in a single damaged  $C_{60}$  molecule. In extended  $C_{60}$  solids, individual cages can be not only polymerized under high pressures but also damaged at very high synthesis temperatures, which are close to the cage stability limit. We point out that the local magnetic moment found in an isolated damaged cage is a part of important ingredients for explaining the existence of magnetic ordering in extended  $C_{60}$  solids.

<sup>8</sup>P. Hohenberg and W. Kohn, *Phys. Rev.* **136**, 864B (1964); W. Kohn and L.J. Sham, *Phys. Rev.* **140**, 1133A (1965).

<sup>9</sup>M.C. Payne, M.P. Teter, D.C. Allan, T.A. Arias, and J.D. Joannopoulos, *Rev. Mod. Phys.* **64**, 1045 (1992).

<sup>10</sup>J.P. Perdew, K. Burke, and M. Ernzerhof, *Phys. Rev. Lett.* **77**, 3865 (1996).

<sup>11</sup>D. Vanderbilt, *Phys. Rev. B* **41**, 7892 (1990).

<sup>12</sup>A.J. Stone and D.J. Wales, *Chem. Phys. Lett.* **128**, 501 (1986).

<sup>13</sup>For tight-binding barrier calculations, see Y.-H. Kim, I.-H. Lee, K.J. Chang, and S. Lee, *Phys. Rev. Lett.* **90**, 065501 (2003).

<sup>14</sup>M. Fujita *et al.*, *J. Phys. Soc. Jpn.* **65**, 1920 (1996); K. Nakada *et al.*, *Phys. Rev. B* **54**, 17 954 (1996); K. Wakabayashi *et al.*, *J. Phys. Soc. Jpn.* **67**, 2089 (1998); K. Kusakabe *et al.*, *Phys. Rev. B* **67**, 092406 (2003).

<sup>15</sup>S. Okada and A. Oshiyama, *Phys. Rev. Lett.* **87**, 146803 (2001).

<sup>16</sup>S. Okada, M. Igami, K. Nakada, and A. Oshiyama, *Phys. Rev. B* **62**, 9896 (2000).

<sup>17</sup>J. Choi, Y.-H. Kim, K.J. Chang, and D. Tománek, *Phys. Rev. B* **67**, 125421 (2003).

<sup>18</sup>Experiments (Refs. 1–3) showed that sample preparation temperatures and pressures lie just below the stability limit of carbon cages, causing the cage collapse followed by graphitization. Thus, the formation of defects including cage opening is very likely to occur under experimental conditions. In thermal equilibrium at 1300 K, the total kinetic energy of a  $C_{60}$  molecule is close to 10 eV.

<sup>19</sup>See S. Baroni, A. Dal Corso, S. de Gironcoli, and P. Giannozzi, <http://www.pwscf.org>